NASA CR- 132399

Mechanical Engineering Department
South Dakota State University
Brookings, S. Dak. 57006

PRIOR-TO-FAILURE EXTENSION OF FLAWS UNDER MONOTONIC AND PULSATING LOADINGS

Inelastic Fatigue

Michael P. Wnuk

(NASA-CR-132399) PRIOR-TO-FAILURE EXTENSION OF FLAWS UNDER MONOTONIC AND PULSATING LOADINGS: INELASTIC FATIGUE Annual Progress Report (South Dakota State Univ.) ~~40~~ p HC $4.00 CSCL 20K

N74-17601

G3/32 Unclas 29271

National Aeronautics and Space Administration
Grant NGR 42-003-006
Annual Progress Report
May 1971

NGR 42-003-006

NASA CR- 132399

Annual Progress Report

PRIOR-TO-FAILURE EXTENSION OF FLAWS UNDER MONOTONIC AND PULSATING LOADINGS (Inelastic Fatigue)

May 1971

This work was supported by
National Aeronautics and Space Administration
Grant NGR 42-003-006

by

Michael P. Wnuk

Department of Mechanical Engineering
South Dakota State University
Brookings, South Dakota

Prior-to-Failure Extension of Flaws Under Monotonic and Pulsating Loadings

by

Michael P. Wnuk

(Abstract)

An equation governing the prior to failure crack propagation is proposed. For a rate-sensitive solid containing two-dimensional crack and subject to the tensile mode of fracture the differential equations are integrated numerically for the loads increasing monotonically in time. The resulting integral curves $\sigma = \sigma(\ell)$ and $\ell = \ell(t)$, i.e. load vs. crack length and length vs. time, indicate that the growth of cracks in the subcritical range is strongly rate dependent.

The fatigue growth, viewed as a sequence of slow growth periods, is simulated on EAI 380 analogue computer. The fourth power law proposed by Paris is confirmed only within certain range of high-cycle fatigue propagation and for a rate-insensitive solid. Otherwise, that is for a more pronounced rate dependency induced by viscosity of a solid and/or in the proximity of the final instability point the growth is markedly enhanced. For sufficiently small ratios of the applied stress intensity range ΔK to the toughness K_c, the suggested fatigue growth law consists of two terms, i.e.

$$\frac{d\ell}{dn} = \frac{\ell_*}{12}\left\{4\left(\frac{\Delta K}{K_c}\right)^4 + Cf^{-1}\left(\frac{\Delta K}{K_c}\right)^2\right\}, \quad \ell_* = \pi K_c^2/8Y^2$$

First term is the familiar Paris expression while the second one accounts for the rate-dependent contribution; f denotes frequency and Y is the yield strength.

Prior-to-Failure Extension of Flaws Under Monotonic and Pulsating Loadings

Part I Basic equations. Monotonic loads.

The catastrophic fracture is often preceded by a quasi-static extension of an initial defect which is too small to be detected. The process of slow propagation occurs at loads below the critical level, and it connot be described in the framework of Griffith-Irwin theory of fracture. In fact the differential equation which governs the subcritical growth in a quasi-brittle solid, [6]

$$M(\sigma,\ell,d\sigma/d\ell) + G(\sigma,\ell) = G_c \tag{1.1}$$

implies possible extension of a pre-existing flaw at incredibly small initial flaw-sizes (or, equivalently, at very low stress levels). It is only at the end of the slow propagation stage, when the "slow growth operator" $M(\sigma,\ell,\frac{d\sigma}{d\ell})$ vanishes, that the Irwin criticality condition is satisfied, i.e.

$$G(\sigma,\ell) = G_c \tag{1.2}$$

or for the linear range of fracture mechanics

$$K(\sigma,\ell) = K_c \tag{1.2a}$$

where G denotes the energy release rate, G_c is the specific fracture energy, $K(\sigma,\ell)$ denotes the stress intensity factor and K_c is the fracture toughness. During an infinitesimal growth the applied stress σ and the corresponding crack length ℓ undergo the change

$$(\sigma,\ell) \rightarrow (\sigma + d\sigma,\ \ell + d\ell) \tag{1.3}$$

This is associated with the plastic energy dissipation absorbed within the end-section of a progressing crack ($\ell \leq x \leq a$) i.e.

$$\delta U = (\delta U)_\ell + (\delta U)_\sigma \tag{1.4}$$

in where

$$(\delta U)_{\ell = \text{const}} = 4Y \frac{d\sigma}{d\ell} \frac{\partial}{\partial\sigma} \int_{\ell}^{a} u(x,\sigma,\ell)\ dx$$

$$(\delta U)_{\sigma = \text{const}} = 4Y\ u(\text{tip}) + 2Y \frac{\partial}{\partial\ell} \int_{\ell}^{a} u(x,\sigma,\ell)\ dx \tag{1.4a}$$

Here $u(x,\sigma,\ell)$ denotes the displacement of a Dugdale crack evaluated within the process zone. The first expression in eqs. (4) is identified as twice the slow growth operator, while the second one is twice the energy release rate. Requirement that the energy balance is satisfied at every instant of the slow propagation stage leads to the governing equation (1); spell out as "Michael plus George equals critical (or crazy) George". The resulting differential equation is valid for the subcritical range of loads

$$\sigma_o \leq \sigma \leq \sigma_c \quad , \quad \text{or}$$

$$K_o \leq K(\sigma,\ell) \leq K_c \tag{1.5}$$

in which σ_o (or K_o) is the propagation threshold, while σ_c (or K_c) is Irwin's critical threshold identified here with the transition to fast propagation. For many ductile solids with well-defined flat "yield shelf" the ratio of the initiation to rapid propagation threshold, K_o/K_c, can be estimated as

$$\frac{K_o}{K_c} \simeq \left(\frac{Y}{E}\right)^{\frac{1}{2}} \simeq \frac{1}{30} \quad \text{(plane stress)} \tag{1.6}$$

where Y is the yield strength and E is the Young modulus. For strain-hardening materials and under high triaxial constraints the above ratio may approach unity, which implies a neglegible amount of slow growth.

Examples of application.

For a two-dimensional Dugdale crack equation (1) reduces to

$$\frac{1}{2}\zeta^2 \frac{d\beta}{d\zeta}[\beta\sec^2\beta - \tan\beta] + \zeta[\beta\tan\beta + \log\cos\beta] = 1 \tag{1.7}$$

while for a penny-shaped crack with an associated Dugdale-type plastic zone it reads

$$\frac{1}{3}\frac{\zeta^2\lambda^3}{(1-\lambda^2)^{3/2}}\frac{d\lambda}{d\zeta} + \zeta\,\frac{1-\sqrt{1-\lambda^2}}{\sqrt{1-\lambda^2}} = 1 \tag{1.8}$$

Here, the applied load σ and the crack length ℓ are normalized as follows

$$\sigma = \begin{cases} \frac{2Y}{\pi}\beta & \text{in}(1.7) \\ Y\lambda & \text{in}(1.8) \end{cases} \qquad \ell = \zeta(\ell_*) = \zeta\left(\frac{\pi K_c^2}{8Y^2}\right) \tag{1.9}$$

For small scale yielding range the above expressions can be expanded into a McLaurin series at $\beta \to 0$ (or $\lambda \to 0$), yielding

$$\frac{d\beta}{d\zeta} = \frac{3}{2}\,\frac{2-\zeta\beta^2}{\zeta^2\beta^3} \quad , \quad \text{plane crack}$$

(1.10)

$$\frac{d\lambda}{d\zeta} = \frac{3}{2}\,\frac{2-\zeta\lambda^2}{\zeta^2\lambda^3} \quad , \quad \text{penny-shaped}$$

Neither of these two equations could have been integrated in a closed form, but as we proceed to show, the numerical (IBM-360) or analogue computer (EAI 380) integration allows one to derive certain simplified rules to be used for prediction of the subcritical growth under

(a) monotonic loadings,

(b) pulsating loadings.

Within the linear domain of fracture mechanics, when yielding is confined to a narrow zone small compared with crack length ($\sigma \ll Y, \ell_* \ll \ell$) an important generalization of eqs. (10) is possible. In such a representation a viscous behavior, in addition to the small scale yielding already represented by equations (10) is accounted for. In this range it is sufficient [6] to replace the time-independent K-factor, $K(\sigma,\ell)$, by the "effective" time-dependent K-factor, namely

$$K_{eff} = K(\sigma,\ell)\ \psi^{\frac{1}{2}}\ (\Delta/\dot{\ell}) \tag{1.11}$$

where ψ denotes the normalized creep compliance $I(t)/I(o)$, $\dot{\ell}$ is the growth rate and Δ denotes the intrinsic opening distance (a material constant). With (11) the equation governing the slow propagation within the subcritical range becomes

$$\begin{aligned} &(\frac{2}{3}\ \zeta\beta + C/\dot{\beta})\ \frac{d\beta}{d\zeta} = \frac{2-\zeta\beta^2}{\zeta\beta^2} \quad , \quad \text{plane crack} \\ &(\frac{2}{3}\ \zeta\lambda + C/\dot{\lambda})\ \frac{d\lambda}{d\zeta} = \frac{2-\zeta\lambda^2}{\zeta\lambda^2} \quad , \quad \text{penny-shaped crack} \end{aligned} \tag{1.12}$$

where C characterizes the rate-sensitivity of the solid

$$\begin{aligned} &C = [\dot{\psi}]_{t=0}\ (\Delta/\ell_*)\ , \text{ or} \\ &C = \Delta[\dot{\psi}]_{t=0}\ (8Y^2/\pi K_c^2) \end{aligned} \tag{1.13}$$

The constant Δ has to be supplied by the experiment.

Two extreme cases result from equations (12) straight forward:

(a) rate insensitive material, in which all the dissipation can be ascribed to plastic time-independent deformation. Then $C \equiv 0$, and eqs. (12) reduces to (10).

(b) highly rate sensitive solid, say a linear visco-elastic matrix containing a crack with a neglegible amount of plasticity present around crack tips. Then eqs. (12) degenerate into

$$(C/\dot{\beta})\ \frac{d\beta}{d\zeta} = \frac{2}{\zeta\beta^2}$$

$$(C/\dot{\lambda})\ \frac{d\lambda}{d\zeta} = \frac{2}{\zeta\lambda^2} \tag{1.14}$$

or

$$\frac{d\zeta}{dt} = C\zeta\beta^2/2$$

$$\frac{d\zeta}{dt} = C\zeta\lambda^2/2 \tag{1.15}$$

It is readily observed that the last two expressions have one common form

$$\frac{d\zeta}{dt} = C \cdot \frac{K_c^2}{K^2(\sigma,\ell)} \tag{1.16}$$

This can be integrated for a prescribed load history $\beta = \beta(t)$, yielding the length of the extending crack as a function of time, $\zeta = \zeta(t)$. Examples of such integration are given in the second part of this report, see Fig. 11.

Numerical Examples

Let us illustrate now how the above equations work. Consider a central crack of half length ℓ roughly ten times greater than the size of the associated plastic zone ℓ_*. The initial crack length is thus

$$\ell = (10)\ell_* = (10)\ (\frac{\pi K_c^2}{8Y^2}) \tag{1.17}$$

and suppose that both the fracture toughness K_c and yield strength Y are known. We want to evaluate the load at which this crack becomes unstable, say σ_c. As the first approximation let us apply Irwin's criterion for failure

$$K(\sigma,\ell) = K_c \tag{1.18}$$

For a central crack contained in a large plate the above equation reads

$$\sigma^2(\pi\ell) = K_c{}^2 \tag{1.19}$$

or, in a dimensionless form,

$$\beta^2\zeta = 2 \tag{1.20}$$

With ζ defined by eq. (17), we obtain

$$\zeta = \frac{\ell}{\ell_*} = 10 \ , \quad \sigma_c = Y\sqrt{\frac{2}{\zeta}} = 0.4472\ Y \tag{1.21}$$

The Griffith-Irwin criterion, therefore, predicts no growth for all loads β less than 0.4472 and the rapid propagation occuring at $\beta_c = 0.4472$ and $\zeta_c = 10$. No slow growth can be accounted for.

Assume now that the solid is quasi-brittle and the propagation threshold K_o is about a quarter of the transition threshold K_c, say $K_o = 0.224\,K_c$. Since

$$\frac{\beta_o}{\beta_c} = \frac{K_o}{K_c} \tag{1.22}$$

we have the starting value of the applied load

$$\beta_o = \beta_c(K_o/K_c) = 0.10 \tag{1.23}$$

This together with $\zeta_o = 10$ provides the initial condition for equations (10) and (12). Numerical integration with the rate sensitivity C assumed to be zero yields the following values of the crack length and the load at instability, say ζ_f and β_f:

$$\zeta_f = 11.4446$$
$$\beta_f = 0.41793 \tag{1.24}$$

Thus we conclude that the catastrophic fracture is preceded by a slow extension of magnitude

$$\Delta\ell = (\zeta_f - \zeta_o)\,\ell_*$$
$$\Delta\ell = (1.44)(\pi K_c^2/8Y^2) \tag{1.25}$$

The final instability occurs at the load

$$\sigma_f = (0.418)Y$$

This is 6.5% less than the load predicted by the Irwin criterion, $\sigma_c = (0.447)Y$.

For larger initial crack lengths and non-zero sensitivity C the discrepancy becomes much more pronounced. Some data substantiating this point are gathered in Table I, while the corresponding graphs are shown in Figs. 1a and 1b.

Table I Instability preceded by the slow growth vs. Irwin's instability (Numbers are generated by eq. (12) and IBM 360).

Initial Length Irwin's Instability		$\zeta_o = 10$ $\beta_c = 0.4472, \zeta_c = 10$		$\zeta_o = 100$ $\beta_c = 0.1414, \zeta_c = 100$		$\zeta_o = 1000$ $\beta_c = 0.0447, \zeta_c = 1000$	
Sensitivity to Loading Rate Ratio	$C/\dot{\beta}$	ζ_f	β_f	ζ_f	β_f	ζ_f	β_f
(ξ_f, β_f) denotes the set of final crack length and applied load at which transition to rapid propagation takes place.	0	11.4446	.41793	102.739	.13952	1004.06	.04463
	.1	11.4856	.41721	102.786	.13950	1004.08	.04463
	1	11.8188	.41147	102.994	.13935	1004.18	.04463
	10	14.1074	.37665	104.979	.13802	1005.26	.04460
	100	24.0228	.28854	117.827	.13028	1014.48	.04440

The amount of slow growth which precedes the catastrophic fracture is distinctly dependent on the initial crack length and ductility of the solid. We have

$$\Delta\ell = f(\zeta_o, C)\,\frac{\pi K_c^2}{8Y^2} \qquad (1.26)$$

or, with K_c replaced by $Y(\pi\delta)^{1/2}\,(\varepsilon_f/\varepsilon_Y)^{(1+N)/2}$

$$\Delta\ell = f(\zeta_o,C)\,\frac{\pi^2}{8}\,\delta(\varepsilon_f/\varepsilon_Y)^{N+1}\ ,\ N\ll 1 \qquad (1.27)$$

The analytic form of the function $f(\zeta_o,C)$ is not known, but for a given ζ_o and C $f(\zeta_o,C)$ can be read out from Fig. 3. The other essential material parameters are the structural size δ ($\ll\ell_*$) and the ratio of strain at failure ε_f to the yield strain ε_Y (=Y/E).

It is obvious that the deviation from Irwin's theory becomes more pronounced for lower toughness threshold levels, for larger initial crack lengths, for enhanced ductility and for materials which are rate sensitive. All the factors mentioned contribute to the inelastic behavior of a solid.

Part II Fatigue in Rate Dependent Solids.

Fatigue crack propagation may be viewed as a sequence of extensions (or steps) of "slow growth" type, each of which occurs while the stress increases during the loading cycle. Therefore the amount of growth produced during one cycle can be computed from eqs. (1.12) by simply integrating both sides of the equation over the load range $\beta_{min} \le \beta \le \beta_{max}$ and regarding the current crack length ζ roughly constant within the single cycle. This latter assumption may not be true for the final stages of fatigue life, where one observes a substantial acceleration of the growth pace, but it certainly is all right for the major portion of the high cycle fatigue life. From eq. (12) we have

$$(d\zeta)_{\text{per cycle}} = \frac{2}{3}\,\zeta^2 \int_{\beta_{min}}^{\beta_{max}} \frac{\beta^3 d\beta}{2-\zeta\beta^2} + \frac{C}{\langle\dot{\beta}\rangle}\,\zeta \int_{\beta_{min}}^{\beta_{max}} \frac{\beta^2 d\beta}{2-\zeta\beta^2} \qquad (2.1)$$

hence

$$\frac{d\zeta}{dn} = \frac{2}{3}\log\frac{2-\zeta\beta^2_{min}}{2-\zeta\beta^2_{max}} + \frac{1}{3}(\beta^2_{min}-\beta^2_{max}) +$$

$$+ \frac{C}{\langle\dot\beta\rangle}\left\{\beta_{min}-\beta_{max} + \frac{1}{\sqrt{2\zeta}}\log\frac{(2+\beta_{max}\sqrt{2\zeta})(2-\beta_{min}\sqrt{2\zeta})}{(2-\beta_{max}\sqrt{2\zeta})(2+\beta_{min}\sqrt{2\zeta}}\right\} \tag{2.2}$$

If the propagation threshold β_o exceeds the minimum stress within a cycle the lower limit of integration in eq. (2.1) should be replaced by β_o. This may considerably alter the propagation rate, see Fig. 2.

For the initial stage of high cycle fatigue progressing at stress intensity remote from the criticality point, the product $\zeta\beta^2$ in the denominator of the integrand of (2.1) can be neglected vs. 2, and we have

$$(d\zeta)_{per\ cycle} = \frac{1}{3}\zeta^2\int_{\beta_o}^{\beta_{max}}\beta^3\,d\beta + \frac{C}{2\langle\dot\beta\rangle}\zeta\int_{\beta_o}^{\beta_{max}}\beta^2\,d\beta \tag{2.3}$$

hence

$$\frac{d\zeta}{dn} = \frac{1}{12}\zeta^2\,[\beta^4_{max}-\beta^4_o] + \frac{C\zeta}{6\langle\dot\beta\rangle}[\beta^3_{max}-\beta^3_o] \tag{2.4}$$

where $\langle\dot\beta\rangle$ denotes the average rate within a cycle.

The range $\Delta\beta = \beta_{max} - \beta_{min}$ does not have to coincide with the integration limits $\beta_o \leq \beta \leq \Delta\beta$, if we allow for the threshold level $\beta = \beta_o$ to lie above the minimum stress in the loading cycle, see Fig. 2.

Fig. 2 The location of the threshold level β_o predetermines the rate of growth.

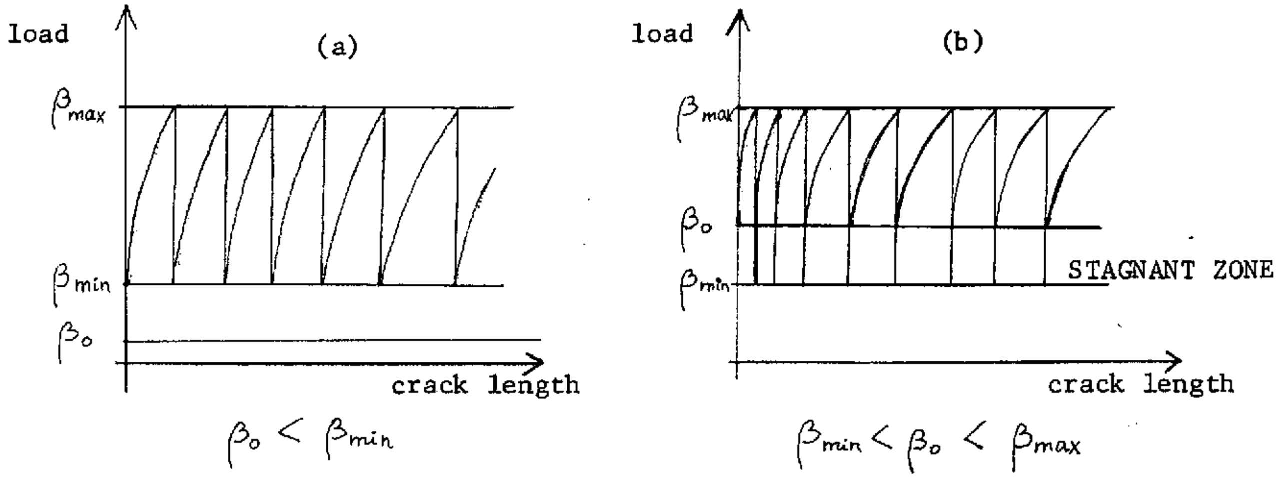

In particular, when one restricts the attention to a zero-to-maximum stress cycle ($\beta_{min} = 0$), and assumes zero threshold $\beta_o = 0$, eq. (2.4) simplifies as follows

$$\frac{d\zeta}{dn} = \frac{1}{12}\,\zeta^2(\Delta\beta)^4 + \frac{C}{6\langle\dot{\beta}\rangle}\,\zeta(\Delta\beta)^3 \qquad (2.5)$$

The first term here can be readily identified with the Paris expression for fatigue crack growth rate, while the second term represents an additional contribution due to the rate sensitivity of a solid. The first term accounts for crack extension in a quasi-brittle solid with no time-effects, and thus it involves the range of K-factor only. The second term decreases when the rate of loading is increased; it does depend on the frequency. The average rate of loading within a single cycle can be related to the frequency as follows

$$\langle\dot{\beta}\rangle = 2f\Delta\beta \qquad (2.6)$$

With this and with $(\Delta\beta)^2\zeta$ replaced by $2(\Delta K/K_c)^2$ eq. (2.6) becomes

$$\frac{d\ell}{dn} = \frac{\ell_*}{3}\left(\frac{\Delta K}{K_c}\right)^4 + \frac{C\ell_*}{12} f^{-1}\left(\frac{\Delta K}{K_c}\right)^2 \tag{2.7}$$

The first term alone gives the well known Paris law*, while the second one tends to increase the pace of growth, at least within the frequency range in which the material is rate dependent (i.e. for f^{-1} comparable to the characteristic relaxation time of a solid).

Computer Simulation of Fatigue Growth.

As ther is no closed form solution to the equation governing crack growth in the subcritical range

$$\frac{d\beta}{d\zeta} = \frac{2-\zeta\beta^2}{\zeta\beta^2\left(\frac{2}{3}\zeta\beta + C/\dot{\beta}\right)} \tag{2.8}$$

We employ the analogue computer technique. The program (see Fig. 4c) has been arranged in such a way that the integration which starts at the initial point (ζ_o, β_o) proceeds up to the point of maximum load in the cycle, then interrupts and reverses to the new "initial" position

$$\zeta_o + \Delta\zeta \ , \ \beta_o$$

where $\Delta\zeta$ denotes the amount of growth within a single cycle. The binary counter recorded the total number of cycles before the critical point was reached. This point is distinguished by zero slope $d\beta/d\zeta$, and it is clearly visible on all photographs

---

* If the range $\Delta k = \Delta K/K_c$ is not very small, the Paris law ought to be replaced by

$$\frac{d\ell}{dn} = \frac{2\ell_*}{3}\left\{\log\frac{1}{1-(\Delta k)^2} - (\Delta k)^2\right\} \tag{2.7a}$$

which depict the final stage of fatigue life. Figures 5 and 6 show an increase of the propagation rate due the time-sensitivity

$$C = \left(\frac{d\psi}{dt}\right)_{t=0} \cdot \Delta/\ell_* \quad , \quad \ell_* = \pi K_c^2/8Y^2 \tag{2.9}$$

of a viscoelastic-plastic solid. In the limit of $C \to 0$ and within the high-cycle range one recovers the fourth power law valid for rate-independent quasi-brittle solid.

Fig. 7 shows three runs at

$$0.1 \leq \beta \leq 0.14 \quad , \quad \Delta\beta = 0.04$$

$$0.1 \leq \beta \leq 0.17 \quad , \quad \Delta\beta = 0.07$$

$$0.1 \leq \beta \leq 0.20 \quad , \quad \Delta\beta = 0.10$$

thus demonstrating shift in the location of the critical point and the change of the rate of growth due to varying stress range. Total numbers of cycles to failure are gathered in Table II. Each run consists of two parts:

$$1 \leq \zeta \leq 10$$

$$10 \leq \zeta \leq 100$$

and then the total number of counts (cycles) is obtained by summing up N(1,10) and N(10,100). The results are repeatable within the accuracy of about 8%.

A somewhat different test is pictured in Fig. 8, where four runs are shown, all at the same range $\Delta\beta = 0.01$ but at different levels of the mean stress (see also Table III). The dependence of N_{TOT} on the stress range, the mean stress and rate sensitivity is summarized in graphs shown in Fig 9 and 10.

Finally, Miner's cumulative damage law is tested in a series of runs performed at varying stress levels. Miner's prediction

(2.10) $$\sum_i \frac{N_i}{N_{if}} = 1$$

N_i = number of loading cycles imposed at mean stress level $\bar{\beta}_i$

N_{if} = number of cycles which would lead to failure if the level $\bar{\beta}_i$ was maintained throughout the test.

turns out to be fairly well satisfied (see Table IV). The agreement deteriorates a little for larger values of the sensitivity parameter and for greater discrepancies between two stress levels used in the program. This trend appears to conform with the deviations from eq. (2.10) reported by investigators who tested Miner's law in the experimental way.

The next test pertains to the limit case of highly rate-sensitive solid in which viscous dissipation is dominant over the plastic work. Then equation (2.8) simplifies to

$$\frac{d\zeta}{dt} = C\,\frac{K_c^2}{K^2(\beta,\zeta)} \quad \text{or} \quad \frac{d\ell}{dt} = C\ell_*\,\frac{K_c^2}{K^2(\sigma,\ell)} \tag{2.11}$$

which in turn can be written as

$$\dot{x} = \frac{\ell_*}{\ell_o}\,C\,\frac{m^2(t)x}{1-m^2(t)x}$$

(2.12)

$$\dot{x} = \frac{\ell_*}{\ell_o}\,C\,\frac{m^2(t)}{x-m^2(t)}$$

Equation (a) above governs the growth of a central crack propagating through a uniformly loaded plate; then

$$K(\sigma,\ell) = \sigma(\pi\ell)^{\frac{1}{2}} \tag{a}$$

while the equation (b) describes the growth induced by the pair of point forces P applied at the center of the crack surface; then

$$K(\sigma,\ell) = P/(\pi\ell)^{\frac{1}{2}} \tag{b}$$

Both σ,(or P) and ℓ vary in time. Function $x(t) = \ell(t)/\ell_0$ is subject to determination, while the load $m(t) = \sigma(t)/\sigma_c$ (or $m = P(t)/P_c$) is given. Both equations (2.12) are then programmed for an analogue computer, see Figs. 4a and 4b, and the resulting integral curves $x = x(t)$ for 3 various loading regimes are shown in Fig. 11. It appears that the pulsating loads (sinusoidal and trapezoidal) produce more rapid growth in the initial stage of propagation than the constant load maintained at the level coinciding with the mean stress within the cycle. Yet another test, not shown here, proved that the randomly pulsating tensile stress produced most severe increase of the flaw size.

Acknowledgments

I wish to thank Professor Davor Juricic who generously donated his time to operate the EAI 380 analogue computer and to whom I owe a number of helpful discussions.

References

1. G. P. Cherepanov, Crack propagation in continuous media, PMM, Vol. 31 No. 3, 1967, p. 476.

2. M. P. Wnuk and W. G. Knauss, Delayed fracture in viscoelastic-plastic solids, Int. J. Solids Structures, 1970, Vol. 6, p. 995.

3. J. M. Krafft, A. M. Sullivan and R. W. Boyle, Effect of Dimensions on fast fracture instability of notched sheets, Crack Propagation Symposium, Cranfiekd, 1961.

4. F. A. McClintock and G. R. Irwin, Plasticity aspects of fracture mechanics, ASTM, Special Technical Publication No. 381, 1964.

5. M. L. Williams, Initiation and growth of visco-elastic fracture, Int. J. Fract. Mech. 1, 292-310, 1965.

6. M. P. Wnuk, Subcritical growth of fracture, Int. J. Fracture Mechanics, in print.

7. F. A. McClintock, On the plasticity of the growth of fatigue cracks, Fracture of Solids, John Wiley & Sons, Inc., New York, 1963.

8. M. P. Wnuk, Effects of time and plasticity on fracture, Brit. J. Appl. Phys., Vol. 2, Ser. 2, 1969, p. 1245.

9. J. R. Rice, Mathematical Analysis in the mechanics of fracture, in "Fracture, an advanced treatise", Vol. 2, Academic Press, New York, 1968.

10. W. G. Knauss and H. Dietmann, Crack propagation under variable load histories in linearly viscoelastic solids, Int. J. Eng. Sci., Vol. 8, 1970, p. 643.

11. J. R. Willis, Crack propagation in viscoelastic media, J. Mech. Phys. Solids, vol. 15, 1967, p. 456.

12. B. V. Kostrov, L. V. Nikitin, L. M. Flitman, Propagation of cracks in viscoelastic solids (in Russian), Fizika Ziemli, No. 7, 1970, p. 20-35.

13. G. P. Marshall, L. E. Culver and J. G. Williams, Crack and craze propagation in polymers: a fracture-mechanics approach, Plastics and Polymers, February 1969, p. 75-81.

14. B. Mukherjee and D. J. Burns, Effect of frequency, mean and range of stress intensity factor on fatigue crack growth in PMMA, paper No. 1727, presented at 1970 SESA Fall Meeting in Boston.

15. F. A. McClintock, Effects of root radius, stress, crack growth and rate on fracture instability, Proc. Royal Society A, Vol. 285, p. 58-72, 1965.

Appendix. Equation of Motion in the Subcritical Range

The rate of work done in separating two surfaces

$$\dot{W} = \int_{\Delta S} T_i \dot{u}_i \, dS \qquad T_i = \text{traction vector}, \quad u_i = \text{displacement vector} \tag{A.1}$$

can be computed from a Dugdale-type model of a plastic zone at the crack tip embedded in a linear viscoelastic solid. If the process zone extends between $x = \ell$ and $x = a$, Y denotes the yield stress and*

$$u = u(x, \sigma(\ell), \ell(t)) \qquad \sigma = \text{stress applied}, \quad 2\ell = \text{crack length}, \quad t = \text{time} \tag{A.2}$$

is the displacement of the crack face, then (A.1) takes the form

$$\dot{W} = 4 \int_{\ell}^{a} Y \cdot \dot{u}(x, \sigma, \ell) \, dx$$

Substituting the rate $\dot{u}$

$$\dot{u} = \frac{\delta u}{\delta t} = \left(\frac{\partial u}{\partial \ell}\right)_{\sigma} \dot{\ell} + \left(\frac{\partial u}{\partial \sigma}\right)_{\ell} \frac{d\sigma}{d\ell} \dot{\ell}$$

into (A.3) and requiring that the energy flow $\dot{W}$ is converted into the surface energy

$$S\dot{E} = 4\dot{\ell}\gamma = 2\dot{\ell}G_c \quad , \qquad G_c = \text{specific fracture energy as defined by Irwin} \tag{A.5}$$

we obtain

$$2Y \int_{\ell}^{a} \left[\left(\frac{\partial u}{\partial \ell}\right)_{\sigma} + \left(\frac{\partial u}{\partial \sigma}\right)_{\ell} \cdot \frac{d\sigma}{d\ell}\right] dx = G_c \tag{A.6}$$

* Note that in the subcritical range load σ is treated as a function of crack length. The function $\sigma = \sigma(\ell)$ is a priori unknown and will be subject to determination.

This can be further reduced to (Wnuk [6]):

$$2Y\ [\frac{\partial}{\partial \ell} + \frac{d\sigma}{d\ell}\frac{\partial}{\partial \sigma}] \int_{\ell}^{a} \dot{u}(x,\sigma,\ell)dx + 2Yu(tip) = G_c$$

which indeed is the equation governing the slow growth in the subcritical range. For a rate-dependent solid we shall have to restrict the validity of the above governing equation to small scale yielding, since only then the viscoelastic displacement $u(x,\sigma,\ell)$ and its increment δu can be expressed as a product of the elastic solution to a given boundary value problem $u^o = u^o(x,\sigma,\ell)$ and the "creep function" $\psi = \psi(t)$, as follows (Wnuk [6]):

$$\begin{aligned} u(x,\sigma,\ell) &= u^o(x,\sigma,\ell) \cdot \psi(\delta t = \Delta/\dot{\ell}) \quad , \quad \Delta = \text{material constant} \\ \delta u(x,\sigma,\ell) &= \delta u^o(x,\sigma,\ell) \cdot \psi(\delta t) + u^o\ \delta\psi \simeq \delta u^o(x,\sigma,\ell) \cdot \psi(\delta t) \end{aligned} \qquad (A.8)$$

Note that the argument of the creep function ψ has been replaced by the time interval δt equal roughly the time used by the crack tip to traverse its own plastic zone. The essential assumptions made here are that the time interval $\delta t = \Delta/\dot{\ell}$ is sufficiently small and that the function ψ does not vary rapidly within the interval δt. This of course implies small scale yielding ($\Delta \to 0$) range, while the rate of loading should be restricted to the "slow" one. These conditions are satisfied when the "inherent opening distance" Δ is much smaller than the characteristic length $\ell_* = \pi K_c^2/8Y^2$, and when an increment of load $\Delta\sigma$ associated with time equal to the representative relaxation time is negligible. With these assumptions equation (A.7) simplifies considerably, and it reads

$$2Y\ \frac{d\sigma}{d\ell}\frac{\partial}{\partial \sigma} \int_{\ell}^{a} u^o(x,\sigma,\ell)dx + 2Yu^o(tip) = \frac{G_c}{\psi(\Delta/\dot{\ell})} \qquad (A.9)$$

Here only the knowledge of elastic solution is implied, and thus both terms in eq.

(A.9) can be identified with the linear fracture mechanics entities, namely

$$2Y \frac{d\sigma}{d\ell} \frac{\partial}{\partial\sigma} \int_{\ell}^{a} u^{o}(x,\sigma,\ell)\,dx = M = \text{slow growth operator} \tag{A.10}$$

and

$$2Yu^{o}(\text{tip}) = G = \text{Irwin's energy release rate} \tag{A.11}$$

The first term M has been recently introduced into the theory of subcritical propagation (reference 6), and may be thought of as a measure of inelastic behavior of a solid. The other term is a well-known Irwin's energy release rate G or Rice's path independent integral $\mathcal{J}$ (or the derivative of the strain energy $G = \frac{1}{2}(\partial U/\partial \ell)_{\sigma}$). It may be readily verified that the Griffith-Irwin instability point is included in the equation (A.9), but it results from it only

i) if the solid is perfectly elastic, then $M \equiv 0$ and $\psi \equiv 1$.

ii) when the final point in the succession of meta-stable states (i.e. for a slowly growing crack) is attained, as then $\frac{d\sigma}{d\ell} = 0$, and again one recovers Irwin's equation $G = G_c$, provided that the matrix is rate-independent. However, if the rate-dependence is there, the simplest form of eq. of motion (A.9) follows for a crack growing under a sustained constant load ($d\sigma = 0$), and it is

$$G(\sigma,\ell) = G_c/\psi(\Delta/\dot{\ell}) \tag{A.12}$$

We shall briefly illustrate how the above equations, in particular (A.9) and (A.12) work. To do so we shall expand the function $\psi(\delta t)$ in the Taylor series around the point $\delta t = 0$ (implying smallness of the interval $\delta t = \Delta/\dot{\ell}$, which is satisfied for $\dot{\ell} > 0$, that is for a crack which already moves. Applied load, therefore, must be <u>above</u> the threshold value). We have

$$\psi(\delta t \to 0) = 1 + \left[\frac{d\psi(\delta t)}{d(\delta t)}\right]_{\delta t=0} \cdot \delta t + \ldots \tag{A.13}$$

or, denoting the derivative $[d\psi(t)/dt]_{t=0} = B$ and recalling that

$$\delta t = \frac{\Delta}{\dot{\ell}} = \frac{\Delta}{\dot{\sigma}} \frac{d\sigma}{d\ell} , \tag{A.14}$$

we get

$$\psi(\delta t) = 1 + B \frac{\Delta}{\dot{\sigma}} \frac{d\sigma}{d\ell} \tag{A.15}$$

for an arbitrary linear viscoelastic solid. Finally computing M (see reference 6) we reduce the governing equation (A.9) to the form

$$G(\sigma,\ell)\left\{1 + \frac{\pi E}{12\eta Y^2} \cdot \frac{\partial G}{\partial \sigma} \left[1 + B \frac{\Delta}{\dot{\sigma}} \frac{d\sigma}{d\ell}\right] \frac{d\sigma}{d\ell}\right\} = \frac{G_c}{1+B \frac{\Delta}{\dot{\sigma}} \frac{d\sigma}{d\ell}} \tag{A.16}$$

in where η equals unity for plane stress and $1-\nu^2$ for plane strain.

The above equation can be linearized if we restrict our attention to the near-critical states only and assume that the powers $(\frac{d\sigma}{d\ell})^2$ and $(\frac{d\sigma}{d\ell})^3$ are negligible vs. $\frac{d\sigma}{d\ell}$. Then (A.16) reduces to

$$1 + \left[\frac{\eta\pi\ell\sigma^2}{E} + B\frac{\Delta}{\dot{\sigma}}\right] \frac{d\sigma}{d\ell} = G_c/G(\sigma,\ell) \tag{A.17}$$

Consider a plane crack contained in a large plate subject to uniform tension, then

$$G(\sigma,\ell) = \eta\sigma^2(\pi\ell)/E \qquad \text{(a)} \tag{A.18}$$

Second configuration of interest is that of a plane crack opened by a pair of point forces applied directly to the crack faces, then

$$G(\sigma,\ell) = \eta P^2/(\pi\ell)E \qquad \text{(b)} \tag{A.19}$$

For these two configurations eq. (A.17) takes the form

$$\left(\frac{2}{3}\zeta\beta + C/\dot{\beta}\right) \frac{d\beta}{d\zeta} = \frac{2-\zeta\beta^2}{\zeta\beta^2} \qquad \text{(a)}$$

$$\left[\frac{2}{3\pi^2}\frac{\beta}{\zeta} + C/\dot{\beta}\right] \frac{d\beta}{d\zeta} = \frac{2\pi^2\zeta - \beta^2}{\beta^2} \qquad \text{(b)}$$

(A.20)

where the dimensionless load β and the dimensionless crack length ζ are defined as follows

$$\beta = \begin{cases} \frac{\pi\sigma}{2Y} & \text{for (a)} \\ \frac{\pi P}{2Y\ell_*} & \text{for (b)} \end{cases} \qquad \zeta = \ell/\ell_*, \; \ell_* = \frac{\pi K_c^2}{8Y^2} \; ; \text{ both cases}$$

Two limit cases which can be treated somewhat easier than the general case are worth mentioning here, and these are

1) $\dot{\beta} = 0$, constant load fracture (static fatigue), for which the equation of motion can be integrated in a closed form.

2) In the other limiting case ($\dot{\beta} \to \infty$, fast loading or time-insensitive matrix) the governing equation simplifies again, since now $C/\dot{\beta} = 0$. Figs.1 a and b show the family of integral curves resulting from eq. (A.20a). They include two extremes of possible behavior:

a) fast loading, cf. the steepest curve;

b) sustained load (zero rate); cf. the horizontal line.

This clearly demonstrates that, all other factors being fixed, the rate of loading and the initial crack length determine the critical stress at which failure will occur. In a similar way the delay time, which elapses between load application and the final instability, is affected by the rate-sensitivity of the solid.

TABLE II

Recorded numbers of cycles to failure at various stress ranges Δ and sensitivities C. The first row gives the number of cycles between $\zeta = 1$ and $\zeta = 10$, the second one refers to $10 \leq \zeta \leq 100$, while the third row gives the total numbers of cycles to failure.

$\beta_{min} = .1$ $\Delta\beta$	β_{max}	RATE SENSITIVITY			
		C = 1.5	1.0	0.5	0
.03	.13	5587	7876	13248	47082
		2084	2415	2884	3978
		7673	10291	16132	51060
.04	.14	3771	5328	8944	30999
		1365	1585	1902	2482
		5146	6913	10846	33481
.05	.15	2713	3846	6457	21491
		937	1088	1311	1713
		3650	4934	7768	23204
.06	.16	2019	2890	4861	17966
		676	782	943	1245
		2695	3672	5804	19211
.07	.17	1563	2250	3728	11978
		498	568	694	920
		2061	2818	4422	12898
.08	.18	1237	1775	2994	9390
		363	424	520	689
		1600	2199	3514	10079
.09	.19	998	1426	2420	7480
		280	323	408	525
		1278	1749	2828	8005
.1	.20	822	1168	1992	6062
		218	255	309	409
		1040	1423	2301	6471

TABLE III

Recorded numbers of cycles to failure at various mean stresses β_{mean} and sensitivities $\underline{C}$. The first row gives the number of cycles between $\zeta = 1$ and $\zeta = 10$, the second one refers to $10 \leq \zeta \leq 100$, while the third row gives the total numbers of cycles to failure.

$\Delta\beta = .01$

Stress level		$\underline{C} = 0.0$	$\underline{C} = 1$	$\underline{C} = 2$
$.12 \leq \beta \leq .13$		107886	19642	10187
		8742	5541	4192
	TOTAL	116628	25183	14379
$.13 \leq \beta \leq .14$		85306	16539	8400
		6989	4454	3344
	TOTAL	92295	20993	11744
$.14 \leq \beta \leq .15$		70533	13819	7112
		5553	3567	2625
	TOTAL	76086	17386	9737
$.15 \leq \beta \leq .16$		58475	11460	6362
		4350	2794	2072
	TOTAL	62825	14254	8434
$.16 \leq \beta \leq .17$		49769	9862	5349
		3406	2176	1655
	TOTAL	53175	12038	7004
$.17 \leq \beta \leq .18$		42351	8579	4732
		2794	1899	1388
	TOTAL	45145	10478	6120
$.18 \leq \beta \leq .19$		36367	7444	4164
		2263	1492	1157
	TOTAL	38630	8936	5321
$.19 \leq \beta \leq .20$		32669	6779	3888
		1875	1278	983
	TOTAL	34544	8057	4871

TABLE IV

Testing the cumulative damage law on the EAI380 analogue computer. Note that the deviation Δ increases for greater sensitivities and discrepancies in the applied stress level.

$\beta_{min} \le \beta \le \beta_{max}$	$\underline{C} = 0$	Δ	$\underline{C} = 1$	Δ	$\underline{C} = 2$	Δ
.19 - .20	$\frac{32669}{34544} = .946$	+ 0.021	$\frac{6779}{8057} = .841$	+ 0.061	$\frac{3888}{4871} = .798$	+ 0.090
.12 - .13	$\frac{8742}{116628} = .075$		$\frac{4454}{20993} = .220$		$\frac{3344}{11744} = .292$	
	total = 1.021		total = 1.061		total = 1.090	
.18 - .19	$\frac{36367}{38630} = .941$	+ 0.017	$\frac{7444}{8936} = .833$	+ 0.045	$\frac{4164}{5321} = .783$	+ 0.068
.13 - .14	$\frac{6989}{92295} = .076$		$\frac{4454}{20993} = .212$		$\frac{3344}{11744} = .285$	
	total = 1.017		total = 1.045		total = 1.068	
.17 - .18	$\frac{42351}{45145} = .938$	+ 0.011	$\frac{8579}{10478} = .819$	+ 0.024	$\frac{4732}{6120} = .773$	+ 0.043
.14 - .15	$\frac{5553}{76086} = .073$		$\frac{3567}{17386} = .205$		$\frac{2625}{9737} = .270$	
	total = 1.011		total = 1.024		total = 1.043	
.16 - .17	$\frac{49769}{53175} = .936$	+ 0.005	$\frac{9862}{12038} = .819$	+ 0.015	$\frac{5349}{7004} = .764$	+ 0.010
.15 - .16	$\frac{4350}{62825} = .069$		$\frac{2794}{14254} = .196$		$\frac{2072}{8434} = .246$	
	total = 1.005		total = 1.015		total = 1.010	
REVERSED ORDER	$\frac{N_i}{N_{if}}, \sum_i \frac{N_i}{N_{if}}$	Δ = deviation from Miner's law	$\frac{N_i}{N_{if}}, \sum_i \frac{N_i}{N_{if}}$	Δ = deviation from Miner's law	$\frac{N_i}{N_{if}}, \sum_i \frac{N_i}{N_{if}}$	Δ = deviation from Miner's law
.12 - .13	$\frac{107886}{116628} = .925$	- 0.021	$\frac{19642}{25183} = .780$	- 0.061	$\frac{10187}{14379} = .708$	- 0.090
.19 - .20	$\frac{1875}{34544} = .054$		$\frac{1278}{8057} = .159$		$\frac{983}{4871} = .202$	
	total = 0.979		total = 0.939		total = 0.910	
.13 - .14	$\frac{85306}{92295} = .924$	- 0.017	$\frac{16539}{20993} = .788$	- 0.045	$\frac{8400}{11744} = .715$	- 0.068
.18 - .19	$\frac{2263}{38630} = .059$		$\frac{1492}{8936} = .167$		$\frac{1157}{5321} = .217$	
	total = 0.983		total = 0.955		total = 0.932	
.14 - .15	$\frac{70533}{76086} = .927$	- 0.011	$\frac{13819}{17386} = .795$	- 0.024	$\frac{7112}{9737} = .730$	- 0.043
.17 - .18	$\frac{2794}{45145} = .062$		$\frac{1899}{10478} = .181$		$\frac{1388}{6120} = .227$	
	total = 0.989		total = 0.976		total = 0.957	
.15 - .16	$\frac{58475}{62825} = .931$	- 0.005	$\frac{11460}{14254} = .804$	- 0.015	$\frac{6362}{8434} = .754$	- 0.010
.16 - .17	$\frac{3406}{53175} = .064$		$\frac{2176}{12038} = .181$		$\frac{1655}{7004} = .236$	
	total = 0.995		total = 0.985		total = 0.990	

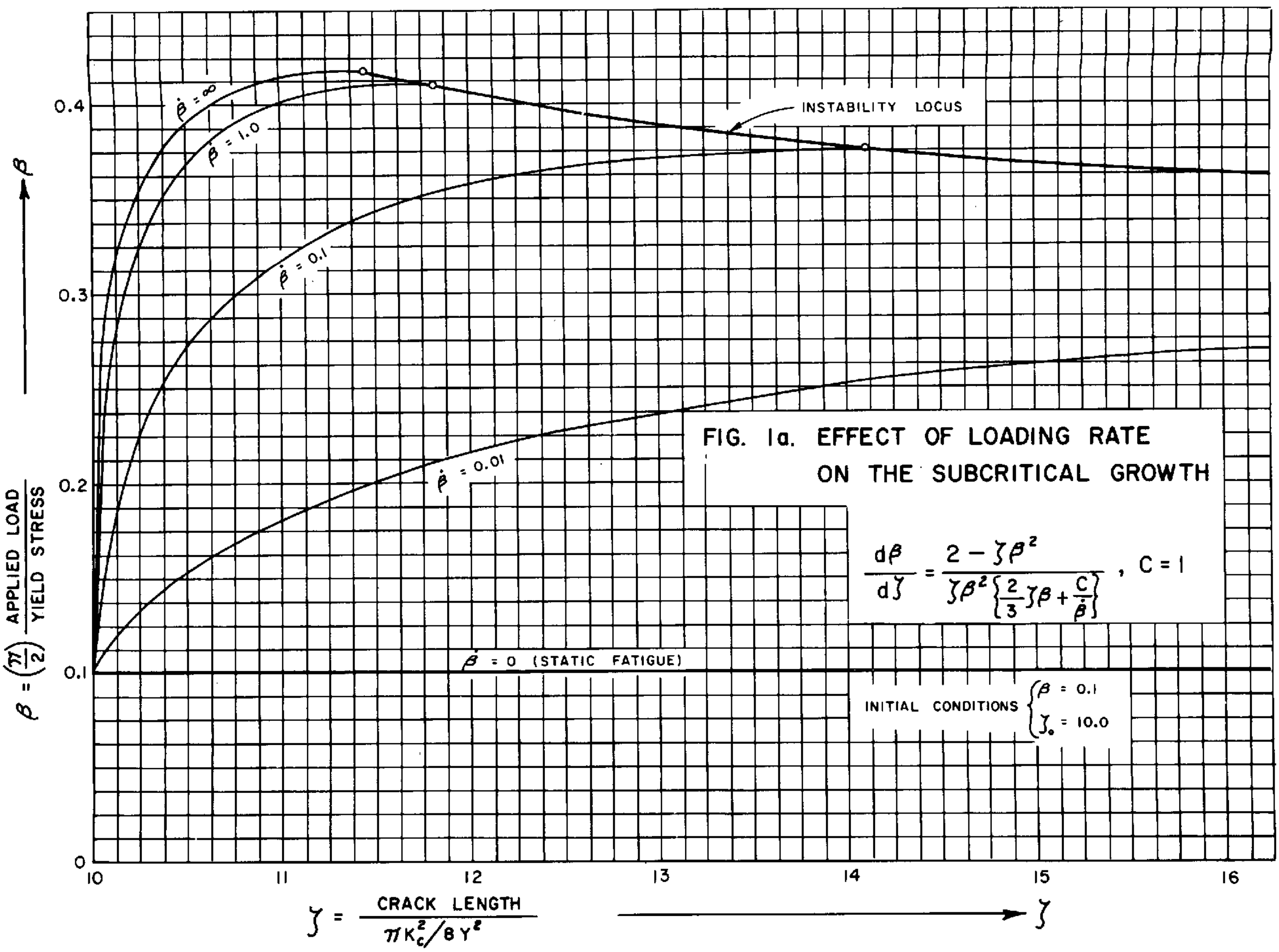

FIG. 1a. EFFECT OF LOADING RATE ON THE SUBCRITICAL GROWTH

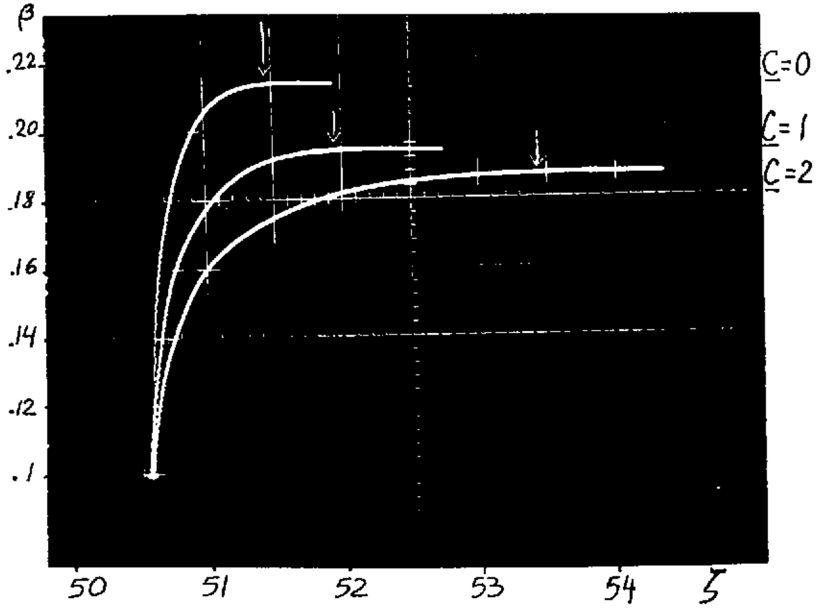

Fig.1b. Subcritical growth induced by a monotonic load at three different rate sensitivities; simulated by the analogue computer EAI 380. Note that the increased internal friction (C)enhances the amount of slow growth. Arrows indicate points of terminal instability.

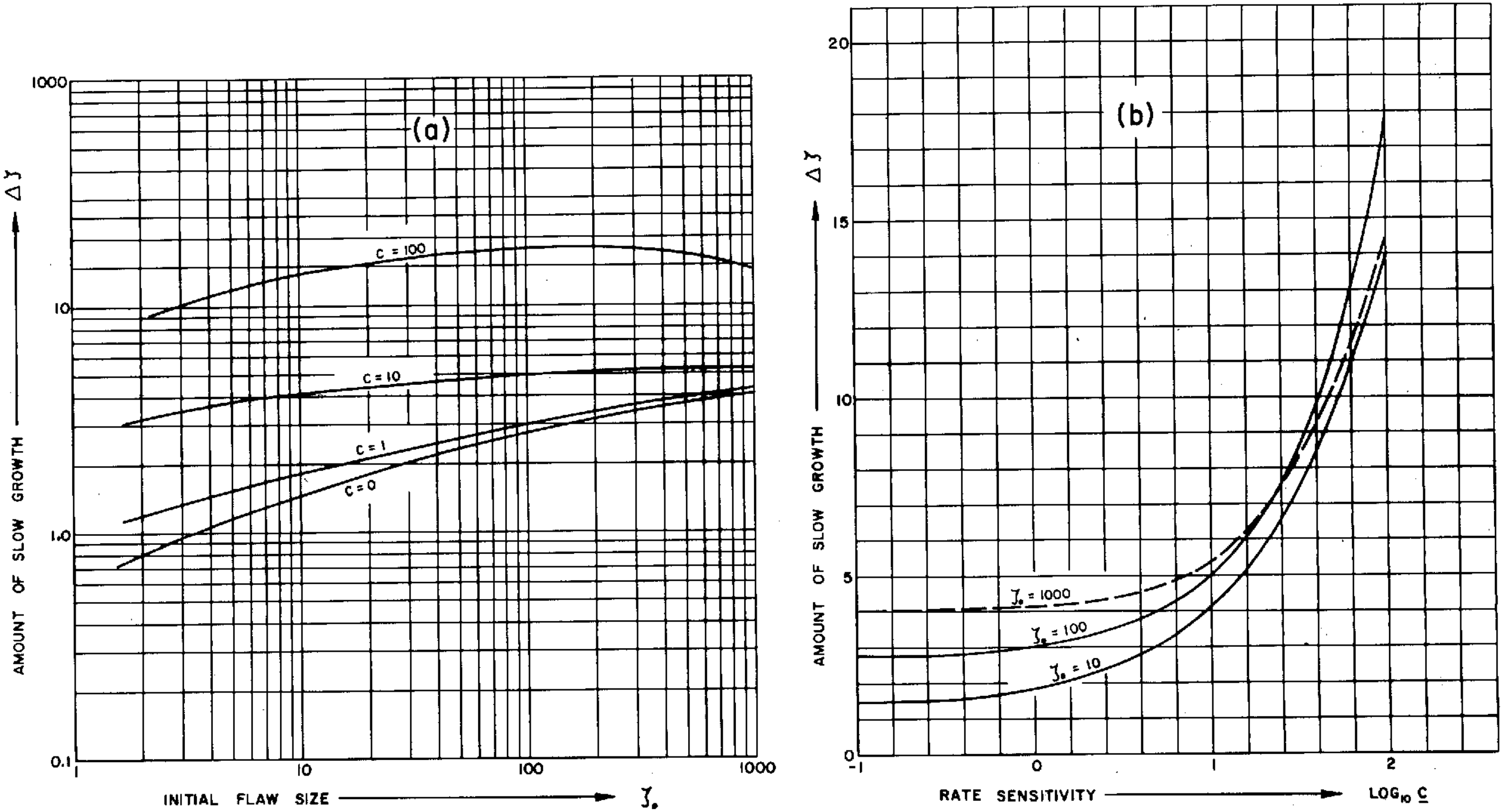

FIG. 3 EFFECT OF THE INITIAL FLAW SIZE (ζ_0) AND THE RATE SENSITIVITY ($\underline{C}$) ON THE AMOUNT OF SLOW GROWTH PRECEDING CATASTROPHIC FAILURE

(ACCORDING TO DATA GENERATED ON EAI 380 ANALOGUE COMPUTOR)

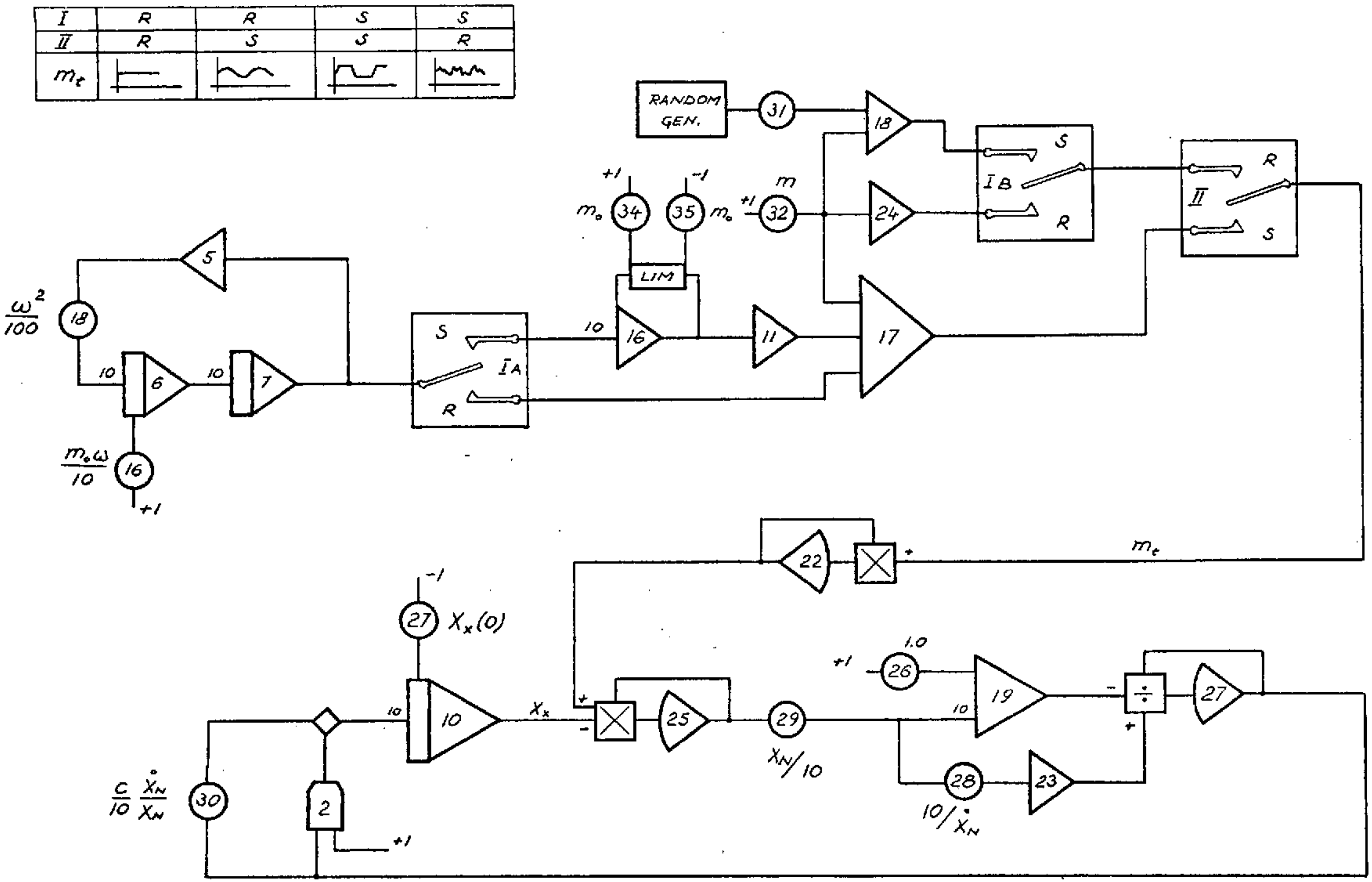

Fig. 4a. Analog computer diagram for integrating equation $\dot{x} = C\,\frac{m^2(t)\,x}{1-m^2(t)\,x}$

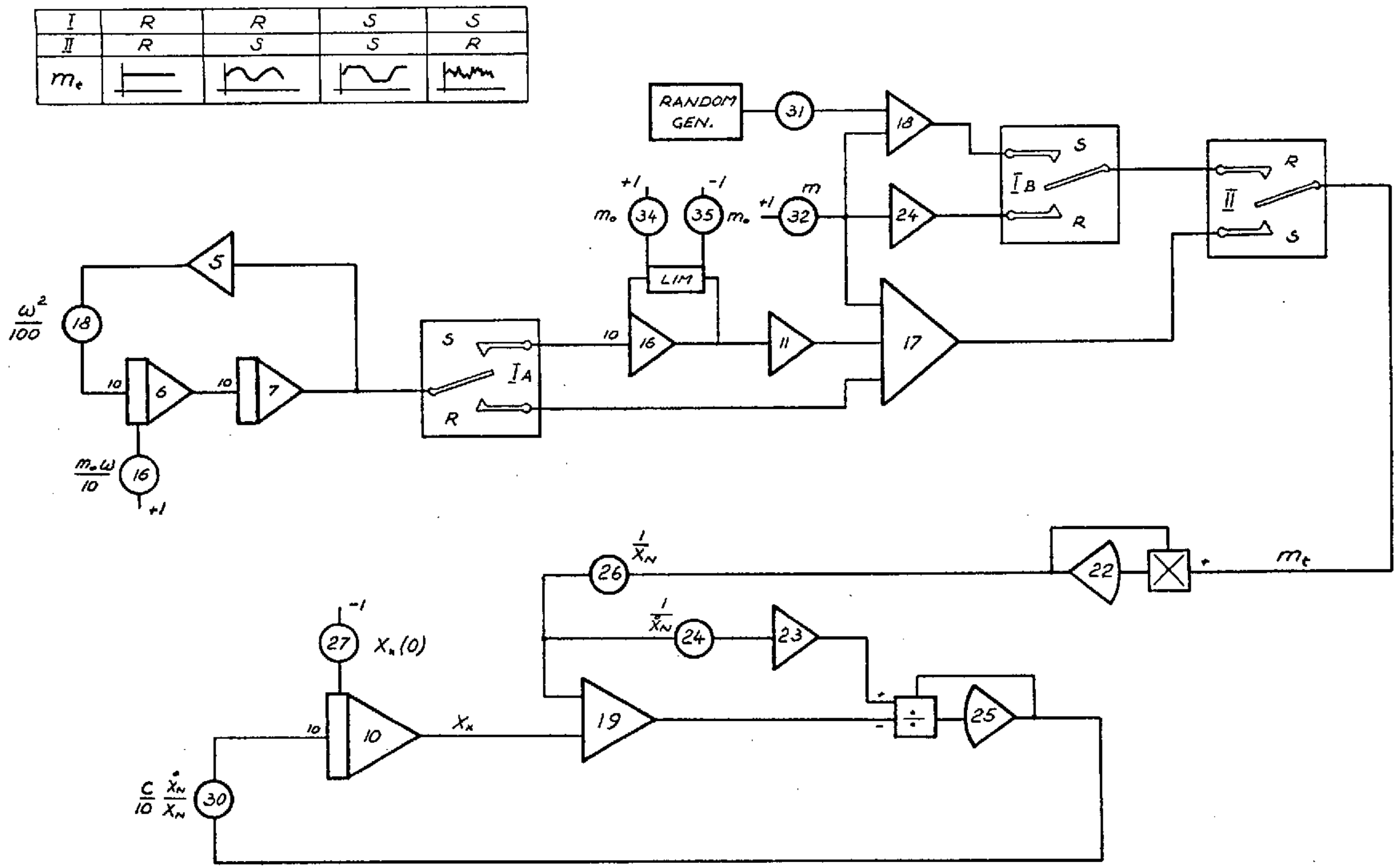

Fig. 4b. Analog computer diagram for integrating equation $\dot{x} = c\,\dfrac{m^2(t)}{x - m^2(t)}$

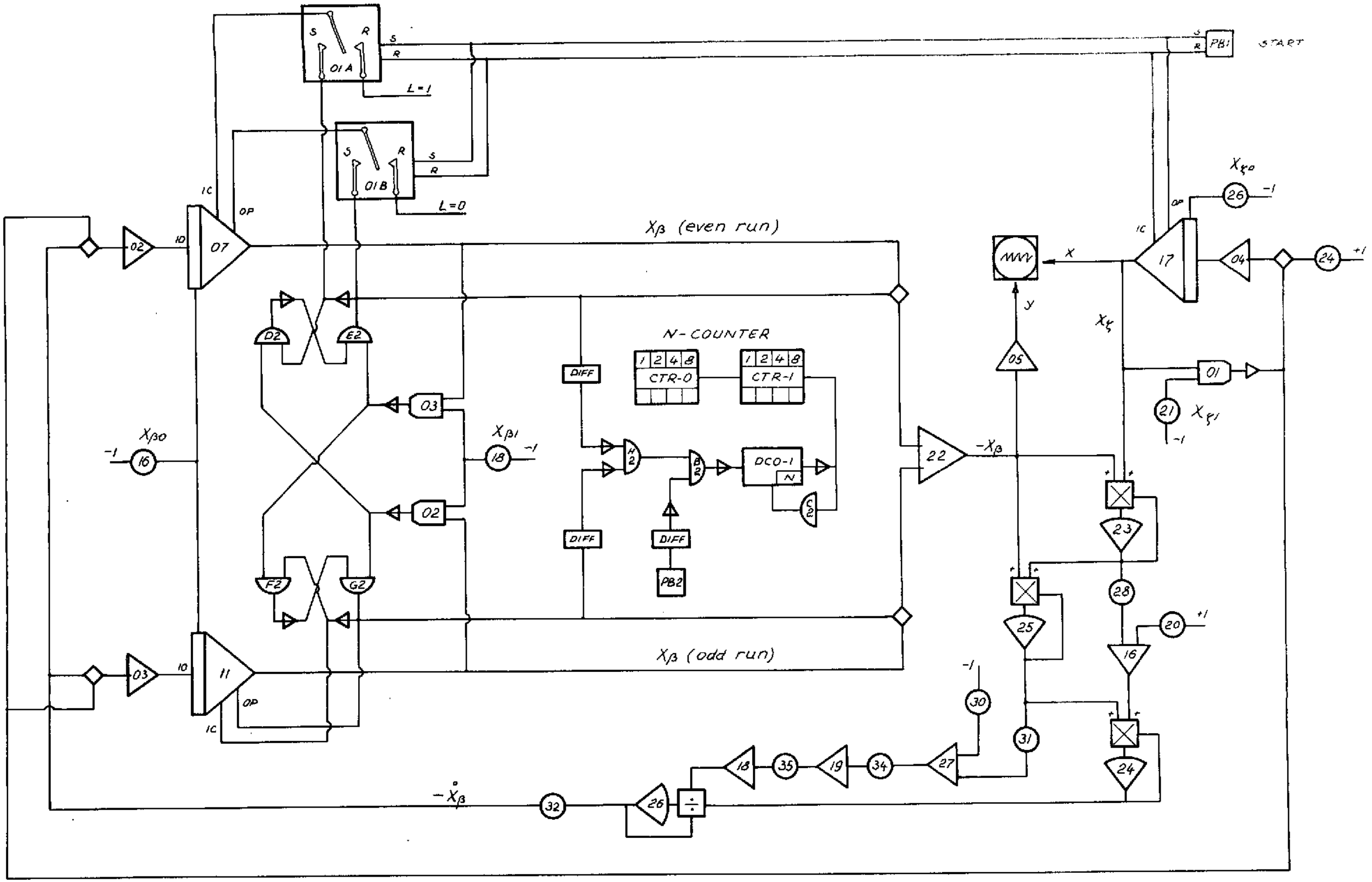

Fig.4c Analogue computer diagram for integrating equation $\frac{d\beta}{d\zeta} = \frac{2 - \zeta\beta^2}{\zeta\beta^2\left(\frac{2}{3}\zeta\beta + C\right)}$ under a pulsating loading regime.

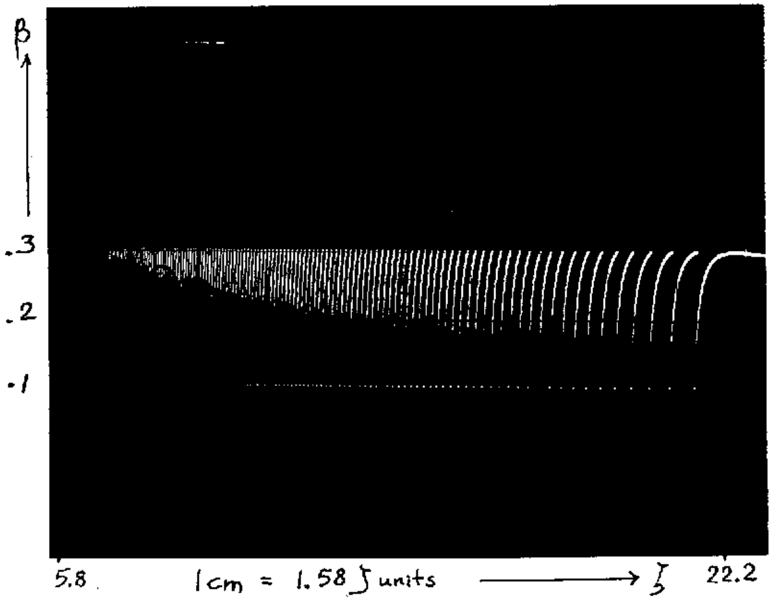

Fig. 5a. Effect of the rate sensitivity $\underline{C} = C/\langle\dot{\beta}\rangle$ on the fatigue crack growth. Increased $\underline{C}$ is equivalent to enhanced sensitivity or/and lower frequency.

Here: $\underline{C} = 0$, initial crack length $\zeta_o = 1$
stress range $0.1 \leq \beta \leq 0.3$
number of cycles not shown = 169
total number of cycles = 426

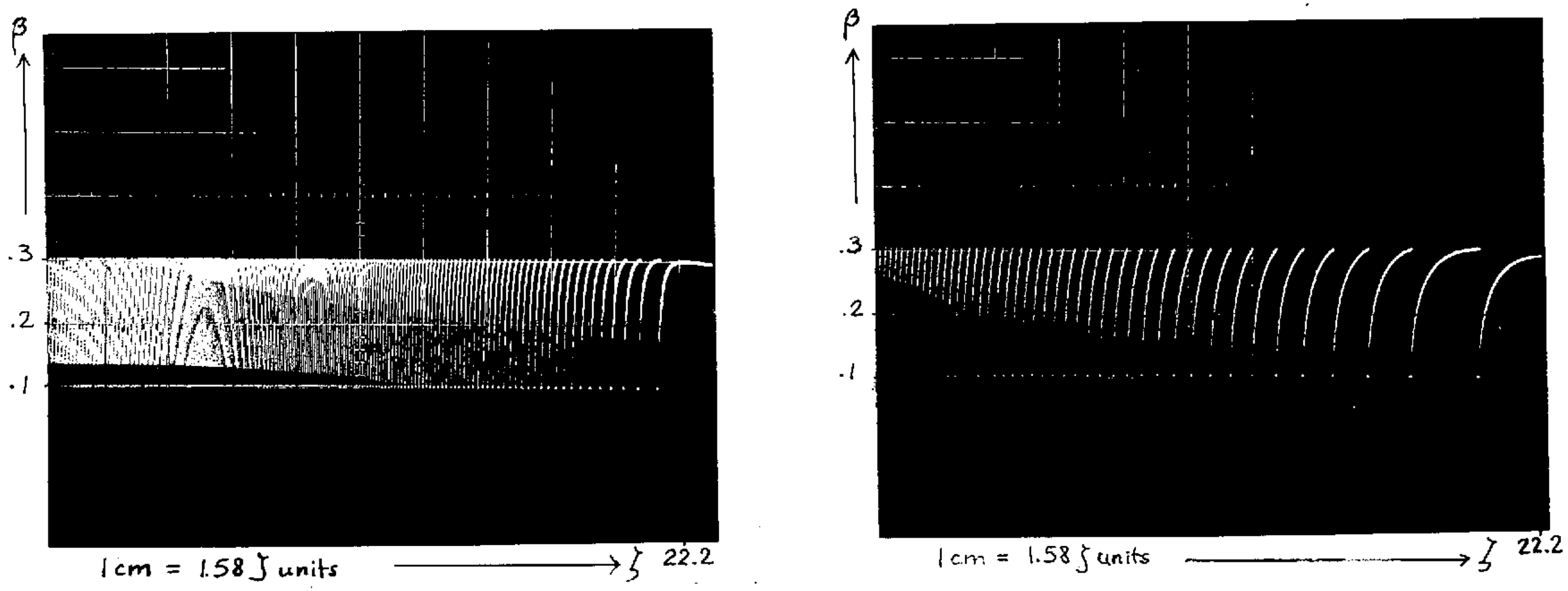

(b) $\underline{C}$ = 0.5, initial crack length ζ_o = 1
stress range $0.1 \leq \beta \leq 0.3$
number of cycles not shown = 160
total number of cycles = 300

(c) $\underline{C}$ = 2.5, initial crack length ζ_o = 1
stress range $0.1 \leq \beta \leq 0.3$
number of cycles not shown = 92
total number of cycles = 132

Fig.5b & c. Effect of rate sensitivity $\underline{C} = C/\langle\dot{\beta}\rangle$ on the fatigue crack growth.
Increased $\underline{C}$ is equivalent to enhanced sensitivity or/and lower frequency.

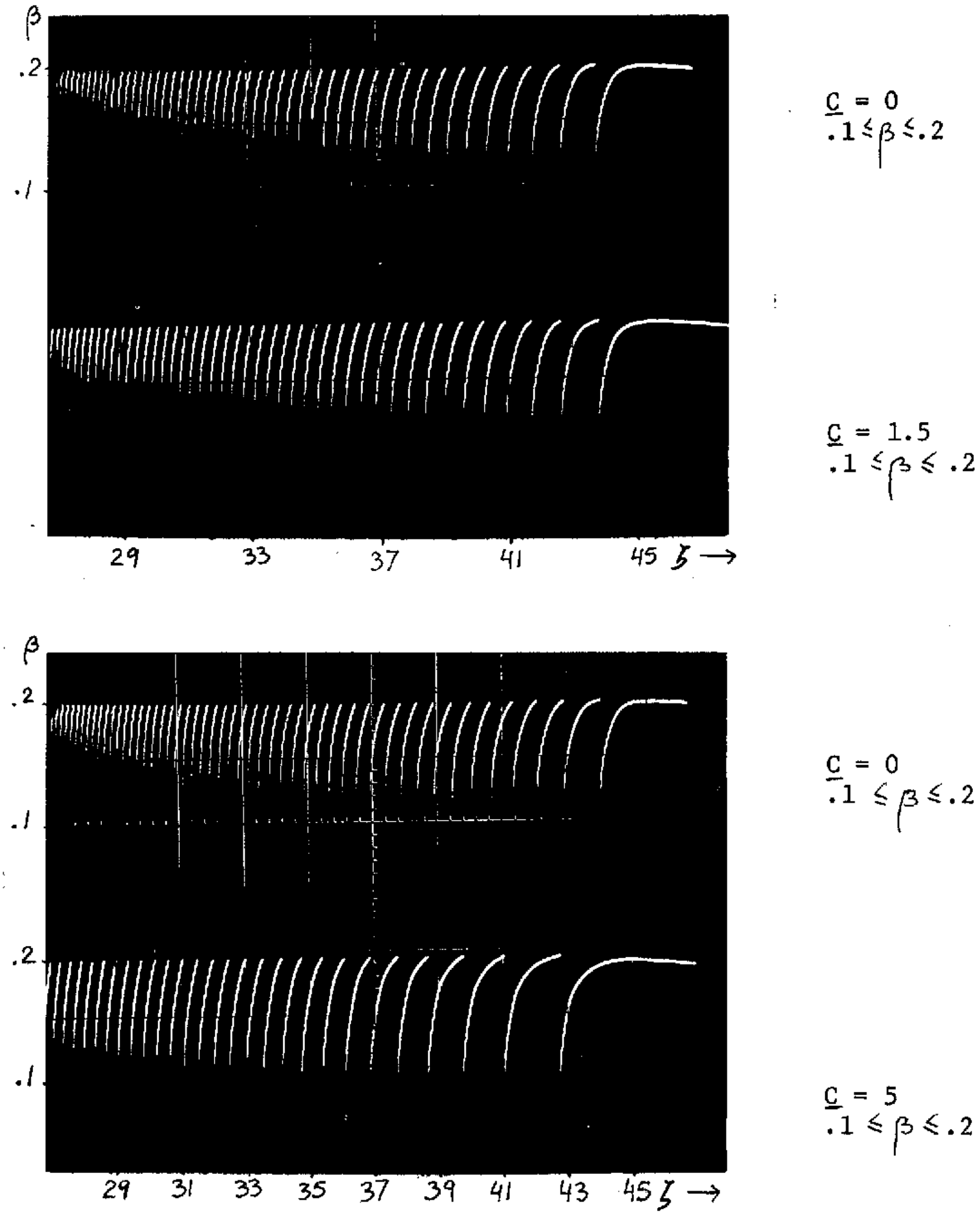

Fig.6 Final stage of fatigue life simulated by the EAI 380 analogue computer. Note the enhanced rate of growth at larger value of sensitivity C.

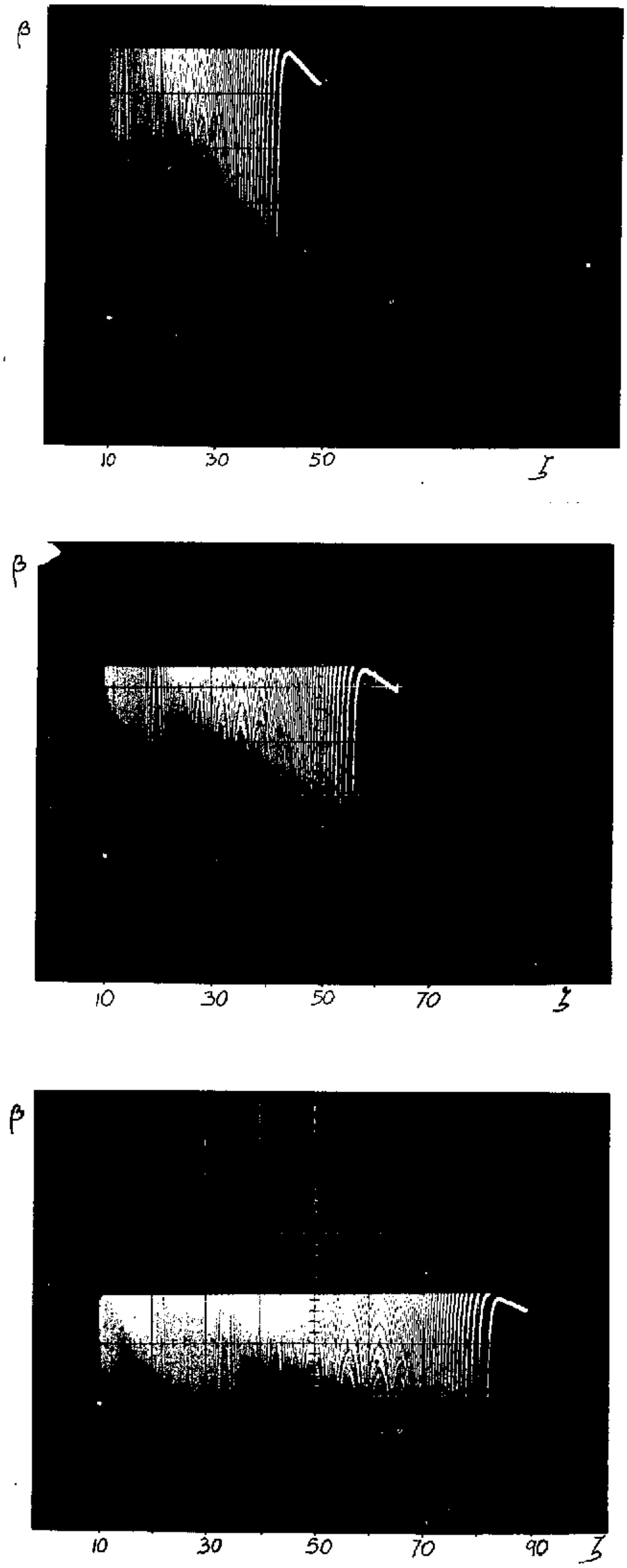

(a) $\underline{C} = 1.5$ $0.1 \leq \beta \leq 0.2$

(b) $0.1 \leq \beta \leq 0.17$

(c) $0.1 \leq \beta \leq 0.14$

Fig.7 Effect of stress range $\Delta\beta$ on the fatigue life (see Table II for the measured numbers of cycles to failure).

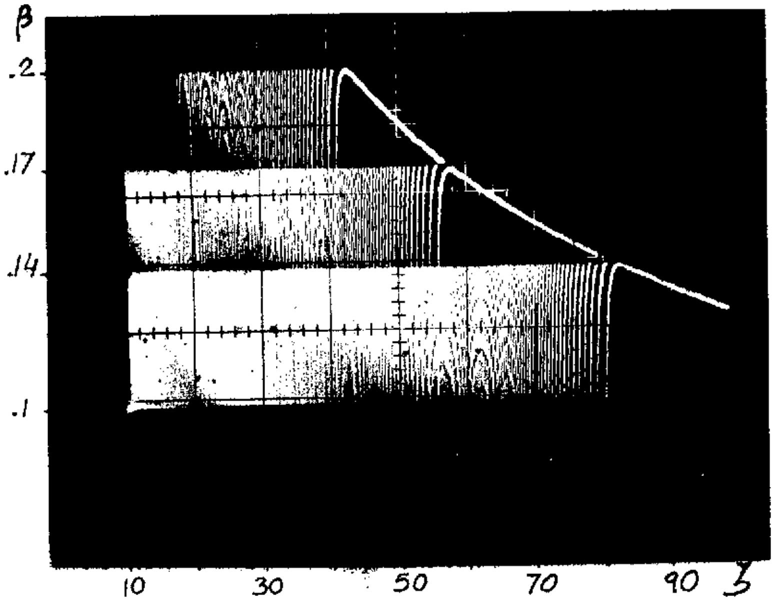

Fig. 7d. Photograph from the oscilloscope screen of runs 7a, 7b and 7c combined.

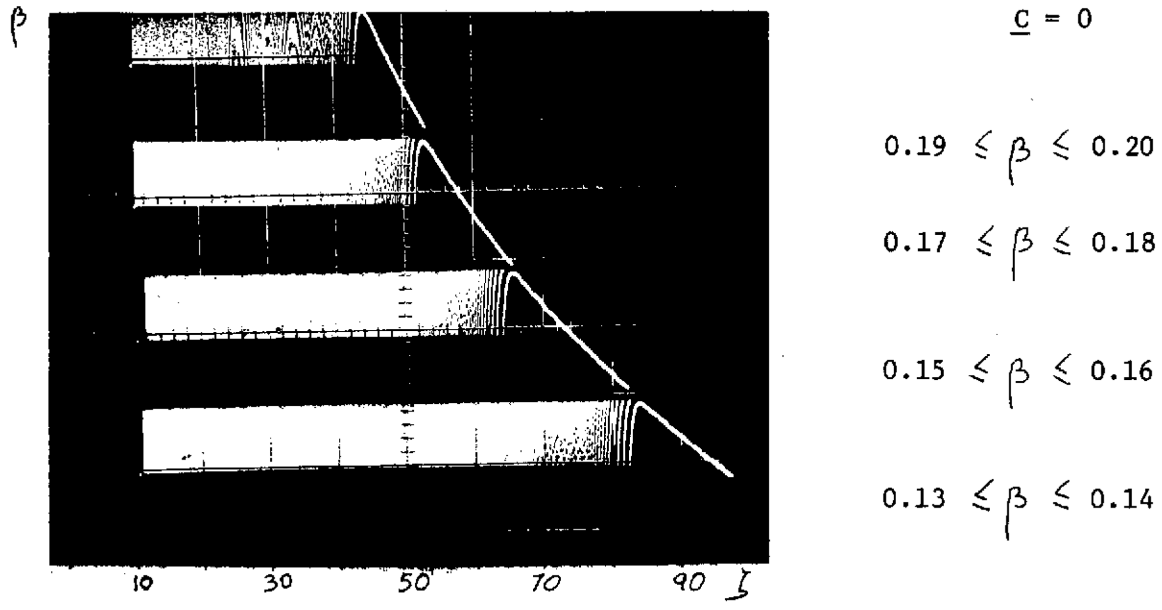

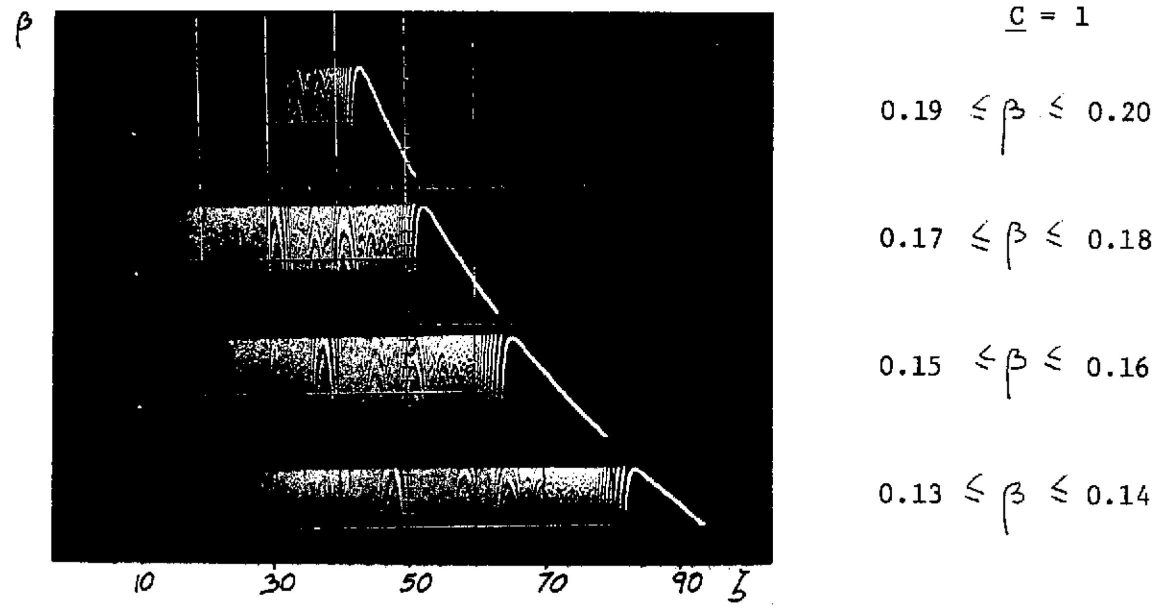

Fig.8 Effect of the mean stress on the fatigue life (see Table III for the measured numbers of cycles to failure).

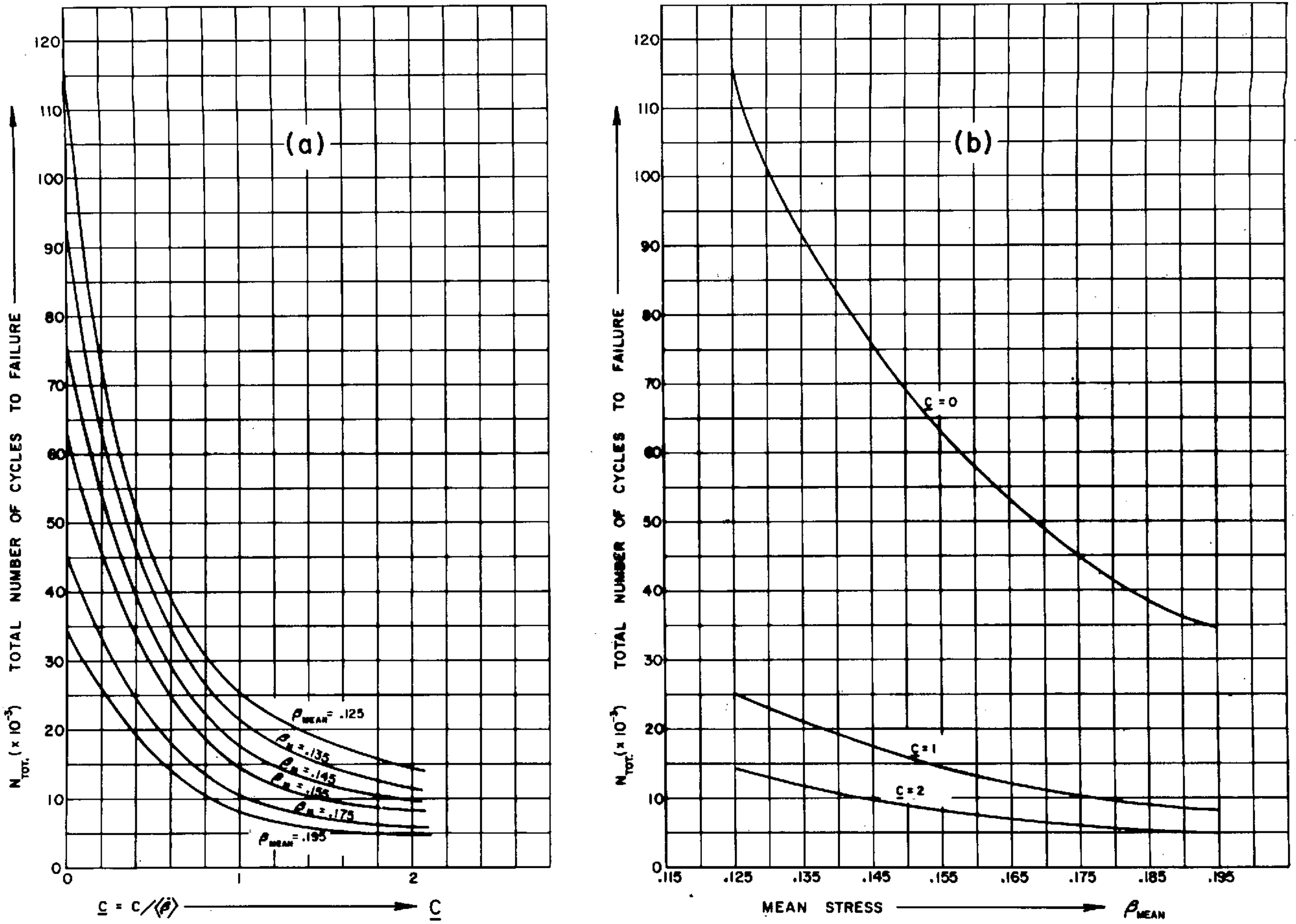

FIG. 9 EFFECT OF THE MEAN STRESS (β_{MEAN}) AND RATE SENSITIVITY (C) ON THE FATIGUE LIFE

(ACCORDING TO DATA GENERATED ON EAI 380 ANALOGUE COMPUTOR)

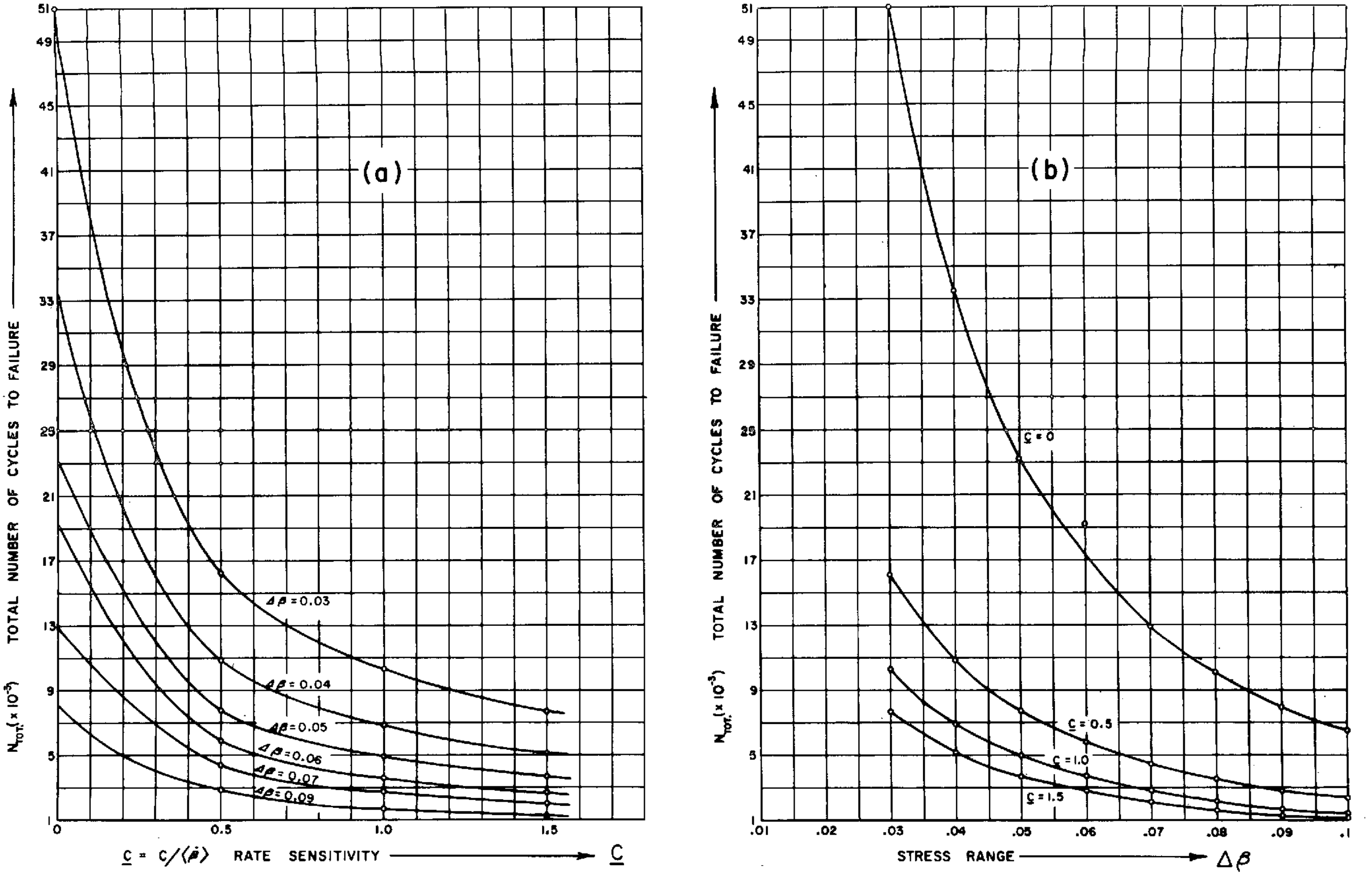

FIG 10. EFFECT OF THE STRESS RANGE (Δβ) AND RATE SENSITIVITY (C) ON THE FATIGUE LIFE

(ACCORDING TO DATA GENERATED ON EAI 380 ANALOGUE COMPUTOR)

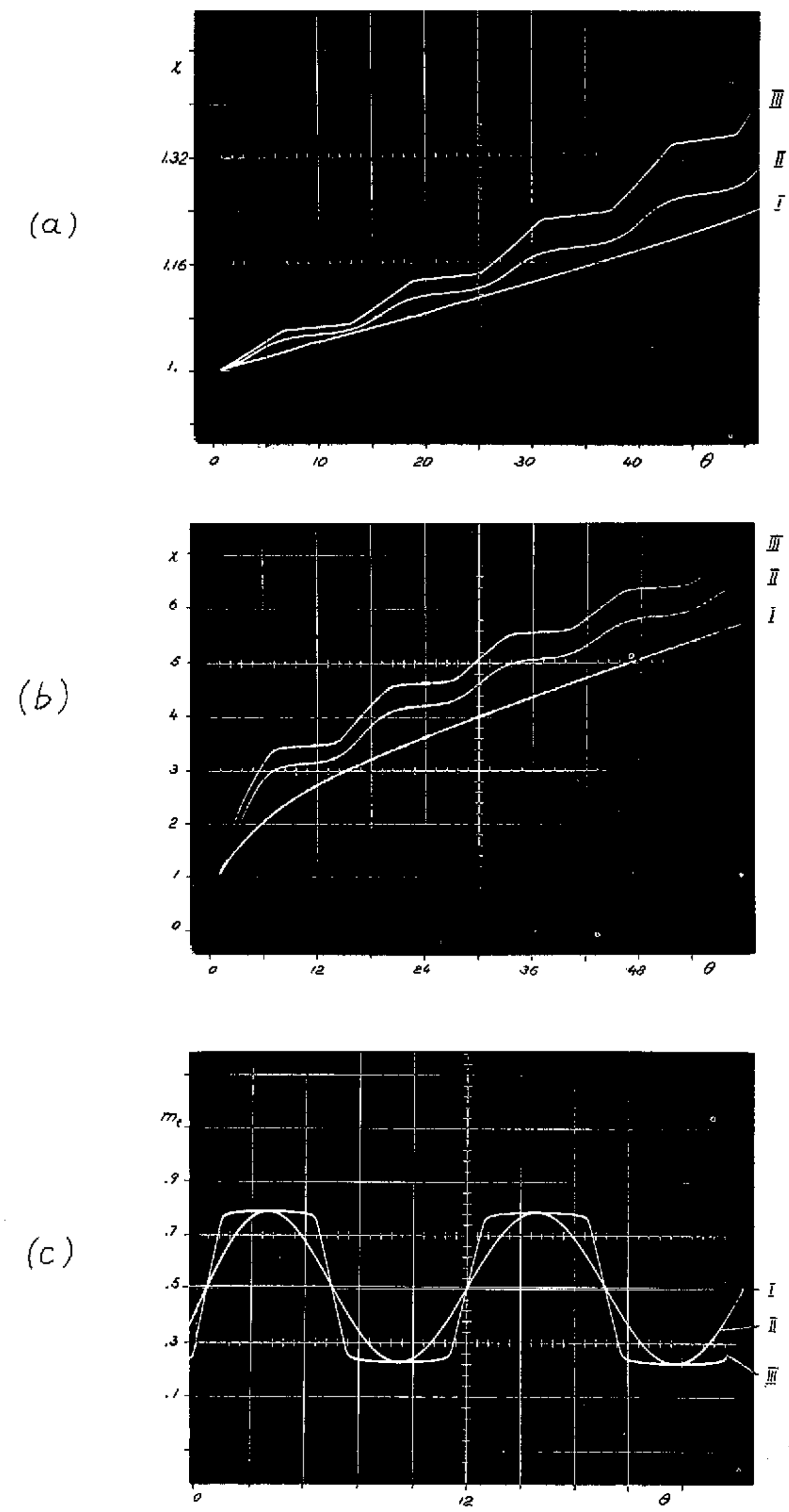

Fig. 11 Subcritical growth of a crack under (a) uniform tensile field, (b) point forces applied directly to crack surface; (c) shows loads imposed. reduced load, crack length and time are: $m = \sigma(t)/\sigma_{crit}$, $x = \ell/\ell_0$, $\theta = t\,\dot{\psi}(0)$.